Novel closed-form resistance formulae for rectangular interconnects*

Chen Baojun(陈宝君)[1, 2, †], Tang Zhen'an(唐祯安)[1], and Yu Tiejun(余铁军)[3]

[1]School of Electronic Science and Technology, Dalian University of Technology, Dalian 116023, China
[2]School of Electronics and Information Engineering, Dalian Jiaotong University, Dalian 116028, China
[3]Department of R&D, Sigrity Inc, Santa Clara, CA 95051, USA

Abstract: Two closed-form formulae for the frequency-dependent resistance of rectangular cross-sectional interconnects are presented. The frequency-dependent resistance $R(f)$ of a rectangular interconnect line or a interconnect line with a ground plane structure is first obtained by a numerical method. Based on the strict numerical results, a novel closed-form formula $R(f)$ for a rectangular interconnect alone is fitted out using the Levenberg–Marquardt method. This $R(f)$ can be widely used for analyzing on-chip power grid IR-drop when the frequency is changing. Compared to the previously published $R(f)$ formula for an interconnect, the formula provided here is more accurate during the frequency transition range. Also for a bigger width to thickness ratio, this formula shows greater accuracy and robustness. In addition, this paper fits out the closed-form $R(f)$ formula for a micro-strip-like interconnect (an interconnect with a ground plane), which is a typical structure in the on-chip or package power delivery system.

Key words: interconnect; resistance; Levenberg–Marquardt method
DOI: 10.1088/1674-4926/32/5/054008 **EEACC:** 2570

1. Introduction

Decades of remarkable technology scaling-down has resulted in the fabrication of integrated circuits (ICs) with smaller feature sizes, higher levels of integration, faster operating frequencies and shorter response times. Although these advances largely benefit IC performance, they also lead to complications that pose significant challenges to on-chip interconnect design, such as delay, power integrity, and signal integrity[1].

In the transient simulations of interconnects, the frequency-dependency of the p.u.l. (per-unit-length) parameter $R(f)$ of transmission lines must be extracted for both on-chip and package interconnects[2]. A simple and accurate interconnect resistance model is the basic requirement in advanced simulation. In order to achieve high simulation efficiency, closed-form formulae are widely used to represent the frequency-dependent resistance of interconnects and some formulae have been presented in Refs. [3–5]. However, after we developed a strict numerical calculation for the interconnection's resistance, we found that the published formulae[3–5] have many limitations. The accuracy is also a concern in the frequency transition range[3]. This is the motivation for the work reported here. We are trying to provide a novel $R(f)$ formula for an interconnect or for an interconnect with ground plane with higher accuracy, bigger line width-to-thickness ratio, and wider frequency range.

In this paper, we first develop a numerical method to calculate the resistance of a rectangular copper line and try to figure out how the final $R(f)$ is changing based on which parameters and in which way. We also give the current distributing in the cross section of the conductor. Then two closed-form formulae are fitted out using the Levenberg–Marquardt method based on the numerical results. The final comparison proves that the formulae have obvious advantages in their accuracy and efficiency in simulation.

2. The numerical method for resistance extraction considering the skin effect and the proximity effect

To capture the interconnect skin effect and proximity effect accurately, we first develop a numerical method to calculate frequency-dependent resistance for a rectangular cross sectional interconnect. To this simple resistance extraction, as shown in Fig. 1, the rectangular line is discretized into many filaments.

The system equation can be generated as

$$V = zI, \tag{1}$$

where V is the per-unit length voltage drop on the line and I is the current density. V and I are the vector with number of

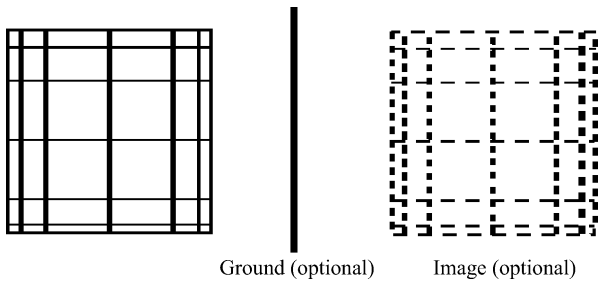

Fig. 1. Rectangular line and its discretization of mesh. Optional ground plane and line image are also shown in the dot-line.

* Project supported by the National Natural Science Foundation of China (No. 90607003).
† Corresponding author. Email: beec98@163.com
Received 17 October 2010, revised manuscript received 18 December 2010

N and $N = N_{\rm p} + N_{\rm g}$, $N_{\rm p}$ and $N_{\rm g}$ are the rectangular line discrization number and its image line's discretization number if you have the optional ground plane. For each filament, it has a resistance r and inductance l, between the different filaments there are inductance coupling. The impedance matrix z can be expressed as

$$[z_{ij}]_{N\times N} = [r_{ij}]_{N\times N} + {\rm j}\omega[l_{ij}]_{N\times N}, \tag{2}$$

where

$$r_{ij} = \begin{cases} \dfrac{1}{\sigma A_i}, & i = j, \\ 0, & i \neq j, \end{cases} \tag{3}$$

and

$$l_{ij} = -\frac{\mu_0}{4\pi A_i A_j}\int_{S_i}\int_{S_j} \ln\left[\left(x-x'\right)^2 + \left(y-y'\right)^2\right] {\rm d}S_i {\rm d}S_j, \tag{4}$$

where A_i is the cross sectional area of filament.

The 2D boundary elemental method (BEM) is used to calculate Eq. (4) and the formula is

$$l_{ij} = \begin{cases} f(x, y/x', y')|_{-0.5a}^{0.5a}|_{-0.5t}^{0.5t}|_{-0.5b}^{0.5b}|_{-0.5t}^{0.5t} \\ \quad + \dfrac{25}{6}\times 10^{-7}, \quad i = j \end{cases} \tag{5a}$$

$$-\frac{\mu_0}{4\pi A_i A_j}\sum_{m}^{N_1}\sum_{n}^{N_2}\sum_{m'}^{N_3}\sum_{n'}^{N_4}\{w_m w_n w_{m'} w_{n'} \times \ln[(x_{im}-x_{jm'})^2 + (y_{in}-y_{jn'})^2]\}, \quad i \neq j. \tag{5b}$$

In Eq. (5b), N_1, N_2, N_3, N_4 are the Gaussian quadrate orders in x and y directions, and $w_m, w_n, w_{m'}, w_{n'}$ are the corresponding weights. To ensure the accuracy, we use Eq. (5a) to calculate the self inductance[6]. Define $f(x)|_x^y = f(y) - f(x)$ and

$$f\,(X,Y) = \frac{\mu_0}{96\pi A_i^2}\left\{\left[X^4 + Y^4 - 6X^2Y^2\right]\ln(X^2+Y^2) - 8XY\left[X^2\tan^{-1}(Y/X) + Y^2\tan^{-1}(X/Y)\right]\right\},$$

$$X = x - x', \quad Y = y - y'.$$

All of the filaments in the rectangular line have the same cross voltage and voltage drop along the line length. The filaments in the rectangular line have their own current, and the summation of all the filaments' current is the final rectangular line's current. Therefore, by solving Eq. (1), one can obtain the current distribution as

$$I = z^{-1}V = yV. \tag{6}$$

Based on the above assumptions, the $N \times N$ filaments l and r matrices can be size reduced to 2×2 matrices by the following approach,

$$[y_{ij}]_{N\times N} = [z_{ij}]^{-1}, \tag{7}$$

$$[Y_{ij}]_{2\times 2} = \begin{bmatrix} Y_{\rm pp} & Y_{\rm pg} \\ Y_{\rm gp} & Y_{\rm gg} \end{bmatrix}, \tag{8}$$

where

$$Y_{\rm pp} = \sum_{i=1}^{N_{\rm P}}\sum_{j=1}^{N_{\rm P}} y_{ij}, \quad Y_{\rm pg} = \sum_{i=1}^{N_{\rm P}}\sum_{j=N_{\rm P}+1}^{N} y_{ij},$$

$$Y_{\rm gp} = \sum_{i=N_{\rm P}+1}^{N}\sum_{j=1}^{N_{\rm P}} y_{ij}, \quad Y_{\rm gg} = \sum_{i=N_{\rm P}+1}^{N}\sum_{j=N_{\rm P}+1}^{N} y_{ij}. \tag{9}$$

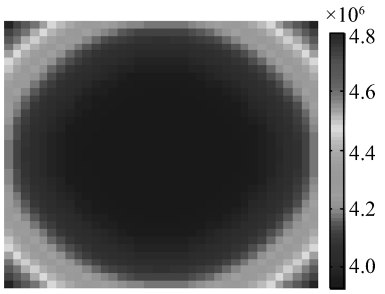

Fig. 2. 2D topographic plot of current density distribution over the cross section of a single line.

Fig. 3. 2D topographic of current density distribution over the cross section of a single line with a ground plane.

Fig. 4. 2D topographic of current density distribution over the cross section of two lines with a ground plane.

Then inverse the 2×2 Y matrix you get the 2×2 Z matrix,

$$[Z_{ij}]_{2\times 2} = R + {\rm j}\omega L = \begin{bmatrix} r_{\rm pp} + {\rm j}\omega l_{\rm pp} & r_{\rm pg} + {\rm j}\omega l_{\rm pg} \\ r_{\rm gp} + {\rm j}\omega l_{\rm gp} & r_{\rm gg} + {\rm j}\omega l_{\rm gg} \end{bmatrix} = \begin{bmatrix} Y_{\rm pp} & Y_{\rm pg} \\ Y_{\rm gp} & Y_{\rm gg} \end{bmatrix}^{-1}. \tag{10}$$

Finally, real(Z_{11}) is the rectangular line's per-unit-length frequency dependent resistance. The technique has been used by some software, such as FastHenry, to calculate the rectangle line's frequency-dependent p.u.l. resistance[7] and the results are accurate.

Figure 2 is the 2D topographic of current density distributing over the cross-section of a single line. Clearly, the current density distributing is symmetric with respect to the $x = w/2$ and $y = t/2$ lines (where w is line width, t is line thickness). Moreover, an explicit edge behaviour is observed. Figures 3–5 are the 2D topographic of current density distributing over the cross-section of conductors with a ground plane. In the presence of a ground, the current density distributing of the conductor can be somewhat different from that of the isolated case due to the proximity effect.

Figure 6(a) presents the frequency-dependent resistance obtained by the numerical method for a single rectangular line. In the picture, we do the normalization which means the picture

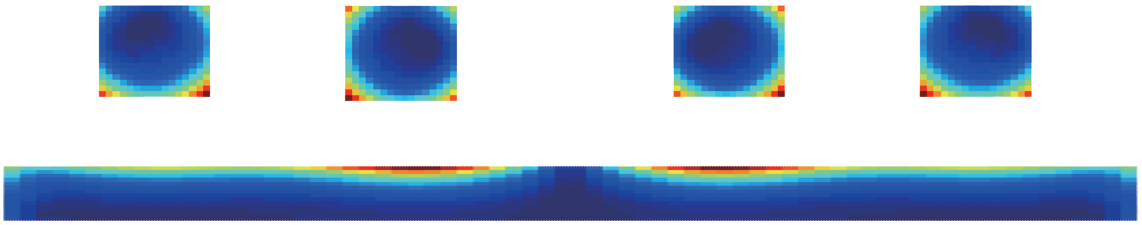

Fig. 5. 2D topographic of current density distribution over the cross section of four lines with a ground plane.

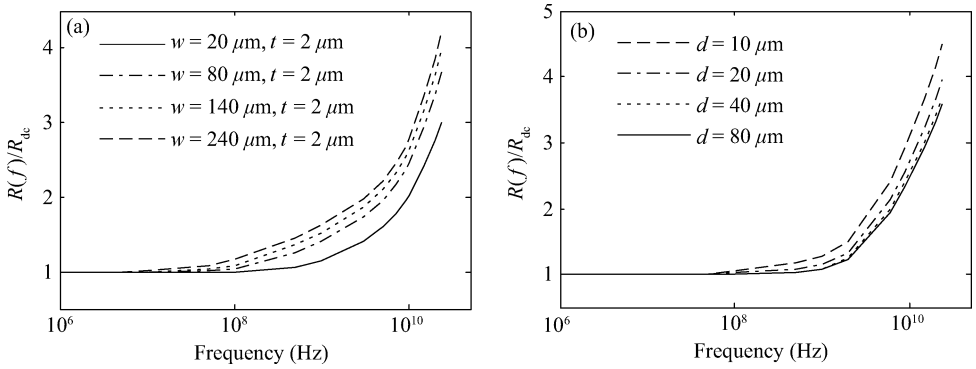

Fig. 6. Normalized frequency dependent per unit length resistance ($R(f)/R_{dc}$).

shows $R(f)/R_{dc}$ instead of $R(f)$. For different w/t (width to thickness) ratios, we can see all of the $R(f)$ convergent to the R_{dc} at low frequency. As the frequency is increased, the wider line first shows skin effects while the fine line shows the skin effect later. Figure 6(b) shows the $R(f)/R_{dc}$ for a single line with a ground plane nearby (where d is the distance between the center of the line and the ground place surface). From the picture, one can see that as the ground plane introduction, the $R(f)$ start increase at early frequency. Also, if the ground plane is closer, the proximity effect is heavier. The line dimension used in Fig. 6(b) is $w = 6\ \mu$m, $t = 4\ \mu$m.

3. The closed-form formulae

3.1. Resistance of single line with rectangular cross section

The frequency-dependent resistance of a single line is represented as

$$\begin{cases} R_{\rm l}^{\rm s}(f) = R_{\rm dc} + n^{\rm s} f + m^{\rm s} f^2, & f < f_{\rm b}, \quad (11a) \\ R_{\rm h}^{\rm s}(f) = {\rm e}^{c^{\rm s} + b_1^{\rm s} \ln(f/f_0) + b_2^{\rm s}[\ln(f/f_0)]^2}, & f \geqslant f_{\rm b}, \quad (11b) \end{cases}$$

where R_{dc} is the direct resistance, f_0 is the break frequency $f_0 = \frac{4}{\pi\mu_0\sigma}\left(\frac{w+t}{wt}\right)^2$, σ is the conductivity and μ is the permeability, and $m^{\rm s}, n^{\rm s}, c^{\rm s}, b_1^{\rm s}, b_2^{\rm s}$ are constants to be described. Equation (11a) is used to compute resistance in the range of low frequency it ensures $R(f)$ equals to R_{dc} at zero frequency, and Equation (11b) corresponds to the high frequency resistance.

To maintain the continuity of the two formulae of $R(f)$ at $f_{\rm b}$, we use two equations to get the parameters $m^{\rm s}, n^{\rm s}$ in Eq. (11a).

$$\left[R_{\rm l}^{\rm s}(f) = R_{\rm h}^{\rm s}(f)\right]\Big|_{f=f_{\rm b}}, \quad (12)$$

$$\left\{\frac{{\rm d}\left[R_{\rm l}^{\rm s}(f)\right]}{{\rm d}f} = \frac{{\rm d}\left[R_{\rm h}^{\rm s}(f)\right]}{{\rm d}f}\right\}\Bigg|_{f=f_{\rm b}}, \quad (13)$$

where Equation (12) shows the continuity of the $R(f)$ and Equation (13) shows the smoothness at the turning points.

Then it can be found that

$$n^{\rm s} = \frac{-R_{\rm h}^{\rm s}(f_{\rm b})\left[b_1^{\rm s} + 2b_2^{\rm s}\ln(f_{\rm b}/f_0) - 2\right] - 2R_{\rm dc}}{f_{\rm b}}, \quad (14)$$

$$m^{\rm s} = \frac{R_{\rm h}^{\rm s}(f_{\rm b})\left[b_1^{\rm s} + 2b_2^{\rm s}\ln(f_{\rm b}/f_0) - 1\right] + R_{\rm dc}}{f_{\rm b}^2}. \quad (15)$$

Dwight[8] introduced the principle of similitude, which states that the ratio of ac to dc resistances for an isolated rectangular strip conductor is a function of two variables, namely, the ratio of strip width to thickness (w/t), and the frequency. So the parameters $c^{\rm s}, b_1^{\rm s}, b_2^{\rm s}, f_{\rm b}^{\rm s}$ are determined by the size of the dimension of the line and their values can be calculated by the Levenberg–Marquardt method.

The Levenberg–Marquardt method[9, 10] is an iterative technique that locates the minimum of a multivariate function that is expressed as the sum of squares of non-linear real-valued functions. It has become a standard technique for non-linear least-squares problems.

Using the Levenberg–Marquardt method, we obtain large numbers of values of $c^{\rm s}, b_1^{\rm s}, b_2^{\rm s}, f_{\rm b}^{\rm s}$. Figure 7 represents the changing rule of $c^{\rm s}$. Obviously, $c^{\rm s}$ is linear to $\ln(w/t)$ and $\ln r_{dc}$. Then we can use a multiple linear function to express $c^{\rm s}$, as shown in Eq. (16). Similarly, we receive Eqs. (17)–(19). Taking Eqs. (16)–(19) into Eq. (11b), we can calculate the resistance in the high frequency range.

$$c^{\rm s} = 0.468 + 0.974 \times \ln R_{\rm dc} + 0.09 \times \ln\frac{w}{t}, \quad (16)$$

$$b_1^{\rm s} = 0.375 - 0.021 \times \ln\frac{w}{t} + 5 \times 10^7 \times wt, \quad (17)$$

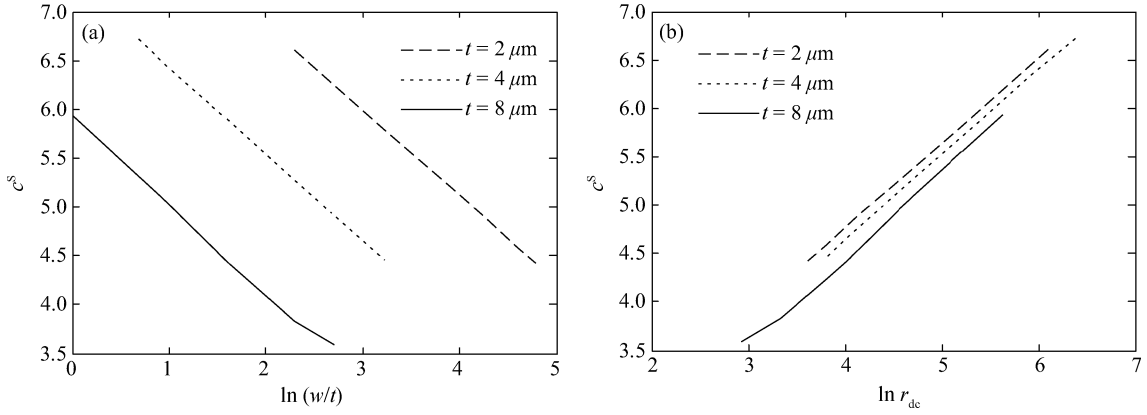

Fig. 7. Parameter c^s is linear to the value (a) $\ln(w/t)$ and (b) $\ln r_{dc}$.

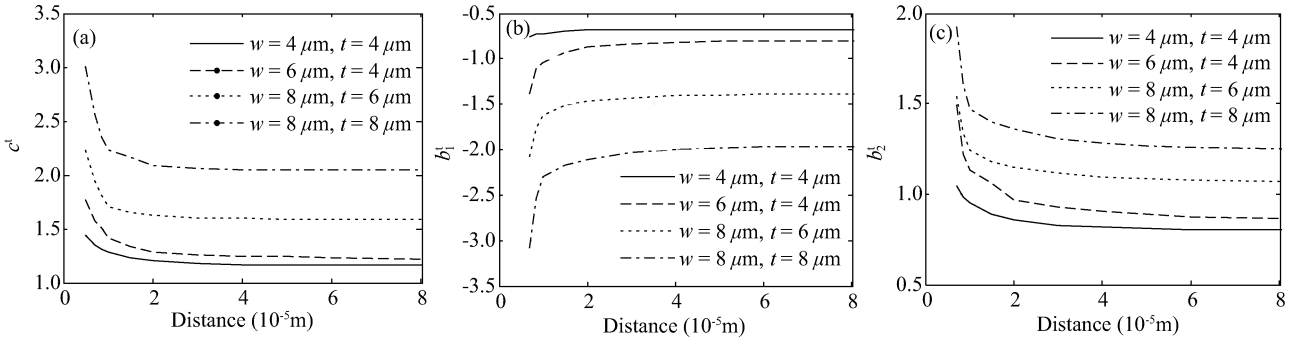

Fig. 8. Values of the parameters are changing with different distance (a) c^t, (b) b_1^t, and (c) b_2^t.

$$b_2^s = 0.048 - 3653.417t, \tag{18}$$

$$f_b = 4 \times 10^7 + 2297833\, R_{dc} + 1300194 \times \frac{w}{t}. \tag{19}$$

The coefficients in Eqs. (16)–(19) are also obtained by the Levenberg–Marquardt method.

So Equation (11a) combined with Eq. (11b) constitutes our final closed-form formula for single rectangular line's p.u.l. $R(f)$ and the parameters in Eq. (11) can be calculated by Eqs. (14), (15) and (16)–(19).

3.2. Formula of line considering the proximity effect

In the presence of a ground or other nearby lines, the resistance of a line can be somewhat different from that of the isolated case due to the proximity effect. So the frequency-dependent resistance is a function of three variables: the dimension of the line, the distance and the frequency.

To consider the ground plane effect, the final rectangular interconnect with a nearby ground plane's frequency dependent p.u.l. resistance $R(f)$ is represented as

$$\begin{cases} R_l^t(f) = R_{dc} + n^t f + m^t f^2, & f < f_b, \quad (20a) \\ R_h^t(f) = R_{dc}\left[c^t + b_1^t \ln p + b_2^t (\ln p)^2\right], & f \geqslant f_b, \quad (20b) \end{cases}$$

where $p = \sqrt{2\mu\sigma f A}$, and A is the cross-section area of the line.

The parameters c^t, b_1^t, b_2^t in Eq. (20b) correspond to the size of the conductor and the distance between the conductor and the ground plane. They are also fitted by the Levenberg–Marquardt method. Figure 8 represents the relation between parameters c^t, b_1^t, b_2^t and the distance from numerical computations. Obviously the curves can be differentiated by dimension, so the parameters $b_{01}, b_{02}, b_{11}, b_{12}, b_{21}, b_{22}$ in Eqs. (21)–(23) can be described by dimension, as shown in Eq. (24)–(29). The derivation of Eq. (20a) is similar to Eq. (11a).

$$c^t = e^{b_{01} + \frac{b_{02}}{d}}, \tag{21}$$

$$b_1^t = -e^{b_{11} + \frac{b_{12}}{d}}, \tag{22}$$

$$b_2^t = -e^{b_{21} + \frac{b_{22}}{d}}, \tag{23}$$

$$b_{01} = -0.119 + 204.304/R_{dc}, \tag{24}$$

$$b_{02} = (0.582 + 1104.015/R_{dc}) \times 10^{-6}, \tag{25}$$

$$b_{11} = -0.884 + 419.6024/R_{dc}, \tag{26}$$

$$b_{12} = (1.584 + 1003.585/R_{dc}) \times 10^{-6}, \tag{27}$$

$$b_{21} = -0.442 + 116.167/R_{dc}, \tag{28}$$

$$b_{22} = (1.827 + 863.608/R_{dc}) \times 10^{-6}, \tag{29}$$

where d is the distance between the center of the line and the ground place surface. The ground plane is regarded as the PEC plane. For the two parameters m^t, n^t in Eq. (20a), their values can also be obtained by the two equations

$$\left[R_l^t(f) = R_h^t(f)\right] | _{f = f_b}, \tag{30}$$

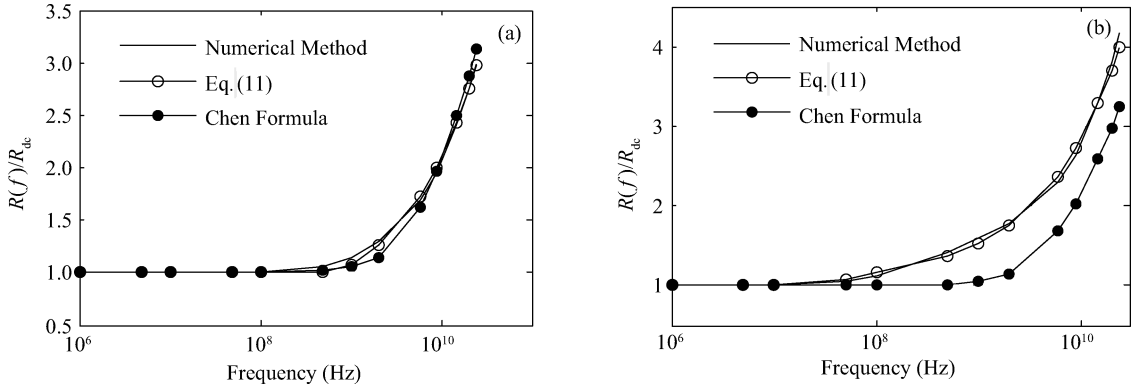

Fig. 9. Comparison $R(f)$ between our Eq. (11), Chen's formula[4] and the numerical method. In (a), the line size is $20 \times 2\ \mu m^2$. In (b), the line size is $200 \times 200\ \mu m^2$.

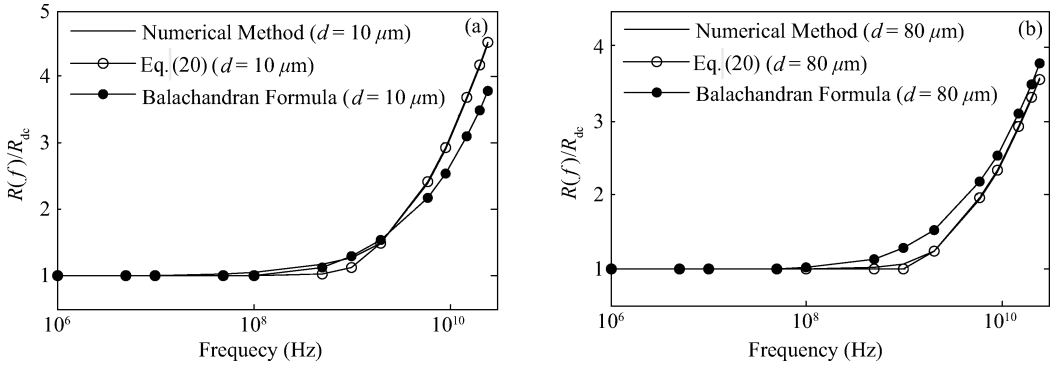

Fig. 10. Comparison $R(f)$ between our Eq. (20), the Balachandran formula[5] and the numerical method. The line size is $6 \times 4\ \mu m^2$.

$$\left\{ \frac{\mathrm{d}\left[R_{\mathrm{l}}^{\mathrm{t}}(f)\right]}{\mathrm{d}f} = \frac{\mathrm{d}\left[R_{\mathrm{h}}^{\mathrm{t}}(f)\right]}{\mathrm{d}f} \right\} \Bigg|_{f=f_{\mathrm{b}}}. \tag{31}$$

And they $(m^{\mathrm{t}}, n^{\mathrm{t}})$ are

$$m^{\mathrm{t}} = \frac{0.5R_{\mathrm{dc}}\left(b_1^{\mathrm{t}} + 2b_2^{\mathrm{t}} \ln\sqrt{2\mu\sigma f_{\mathrm{b}} A} + 2\right) - R_{\mathrm{h}}^{\mathrm{t}}(f_{\mathrm{b}})}{f_{\mathrm{b}}^2}, \tag{32}$$

$$n^{\mathrm{t}} = \frac{2R_{\mathrm{h}}^{\mathrm{t}}(f_{\mathrm{b}}) - 0.5R_{\mathrm{dc}}\left(b_1^{\mathrm{t}} + 2b_2^{\mathrm{t}} \ln\sqrt{2\mu\sigma f_{\mathrm{b}} A} + 4\right)}{f_{\mathrm{b}}}. \tag{33}$$

So Eq. (20a) combined with Eq. (20b) constitutes the final closed-form formula for a single rectangular line with a nearby ground plane's frequency-dependent p.u.l. $R(f)$ and the parameters in Eq. (20) can be calculated by Eqs. (21)–(29) and (32)–(33).

4. Results and discussion

Equation (11) is an explicit expression that contains the frequency and the line size as variables. To validate the formula, we compare it with the numerical results and Chen formula[4].

Figure 9 shows the comparison between the different resistance values of a single line: the proposed formula (11) results, Chen formula[4] results and the numerical results. The numerical results are regarded as the standard true results. From the picture, one can see our proposed formula results always agree well with the numerical results in all frequency ranges and with different dimensions. The maximum relative error is less than 5%. While for Chen formula[4], for 20 μm width and 2 μm thickness line, it matches well with the numerical results (Fig. 9(a)) with about 10% error in the transition frequency range; but in the case of a 200 μm width and 2 μm thickness line, Chen's formula results are far away from the numerical results which show more than 50% error in Fig. 9(b). These experiments show that our equation (11) is valid in the larger line geometry range and is much better than Chen's formula.

Balachandran[5] derived a formula to calculate the resistance while taking the ground plane into account. Figure 10 compares the frequency-dependent resistances considering the proximity effect with Eq. (20) proposed in this paper and the Balachandran formula[5]. It can be seen that when the distance between the conductor and the ground changes, Equation (20) agrees fairly well with that from numerical computation. Also, Figure 10 shows our formula's accuracy advantages over the Balachandran formula in large line w/t ratio ranges.

5. Conclusion

In this paper, a new formula for frequency-dependent resistance of a rectangular cross-sectional conductor is presented in Eq. (11); frequency-dependent resistance of rectangular line with a nearby ground plane is presented in Eq. (20). Both closed-form formulae are fitted out in the Lev-

enberg–Marquardt method based on the accurate numerical results. Compared to the former formulae found in the literature, these two formulae have obvious advantages in the accuracy and application dimension varying ranges. The proposed formulae can be used widely in IC, package and board level CAD simulation for power or signal integrity.

References

[1] Wong B P, Mittal A, Cao Y. Nano-CMOS circuit and physical design. New York: John Wiley & Sons, 2004

[2] Tsuk M J, Kong J A. A hybrid method for the calculation of the resistance and inductance of transmission lines with arbitrary cross sections. Microwave Theory and Techniques, 1991, 39(8): 1338

[3] Clayton R P. Analysis of multiconductor transmission lines. New York: John Wiley & Sons, 1994

[4] Chen H, Fang J. Modeling of impedance of rectangular cross-section conductors. Electrical Performance of Electronic Packaging, 2000: 159

[5] Balachandran J, Brebels S, Carchon G. Compact broadband resistance model for microstrip transmission lines. Electrical Performance of Electronic Packaging, 2004: 83

[6] Weeks W T, Wu L L, McAllister M F, et al. Resistive and inductive skin effect in rectangular conductors. IBM Journal of Research and Development, 1979, 6: 652

[7] Wei Hongchuan, Yu Wenjian, Yang Liu, et al. Fast inductance and resistance extraction of 3-D VLSI interconnects based on the method of K element. Acta Electronica Sinica, 2005, 8: 1635

[8] Faraji-Dana R, Chow Y. Edge condition of the field and AC resistance of a rectangular strip conductor. Microwaves, Antennas and Propagation, 1990, 137(2): 133

[9] Madsen K, Nielsen H B, Tingleff O. Methods for non-linear least squares problems. Informatics and Mathematicl Modeling Technical University of Denmark, 2004: 24

[10] Chen Baojun, Tang Zhen'an, Yu Tiejun. A novel closed-form resistance model for trapezoidal interconnects. Journal of Semiconductors, 2010, 31(8): 084011